

# Flow loss characteristics in parallel confluence sections of tunnels

Xin ZHANG, Hao HE, Xiaofeng CHEN, Yachao LI, Tianhang ZHANG,  
Yuehui WANG, Kai ZHU, Ke WU

Cite this as: Xin ZHANG, Hao HE, Xiaofeng CHEN, Yachao LI, Tianhang ZHANG, Yuehui WANG, Kai ZHU, Ke WU, 2025. Flow loss characteristics in parallel confluence sections of tunnels. *Journal of Zhejiang University-SCIENCE A (Applied Physics & Engineering)*, 26(7):666-678.

<https://doi.org/10.1631/jzus.A2400405>

# Research Objective

Local loss for direct dividing section (Numerous studies have been conducted)



Local loss for parallel converging section (Our Research Focus)

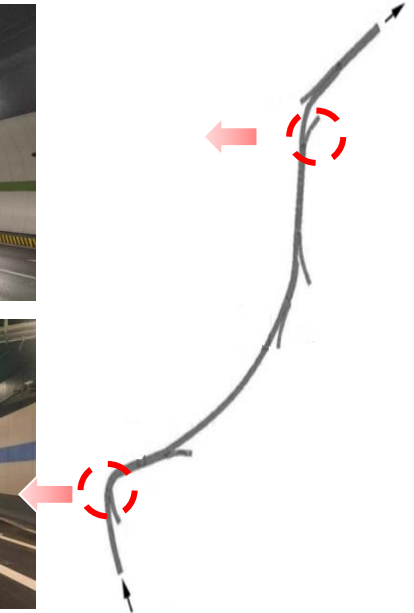
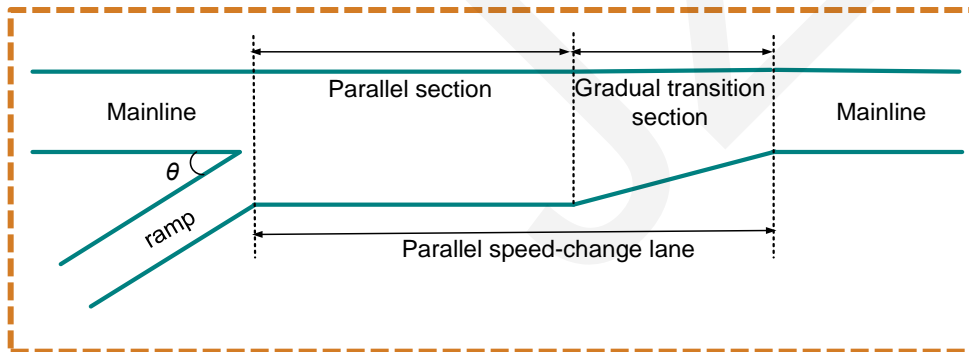
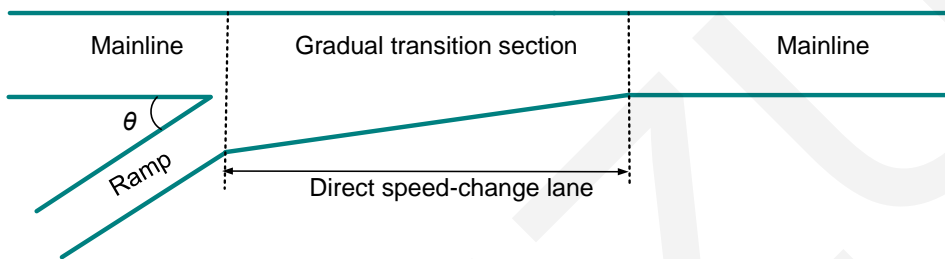
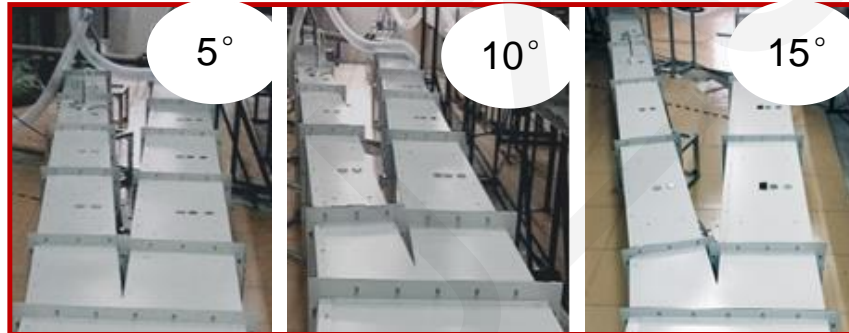
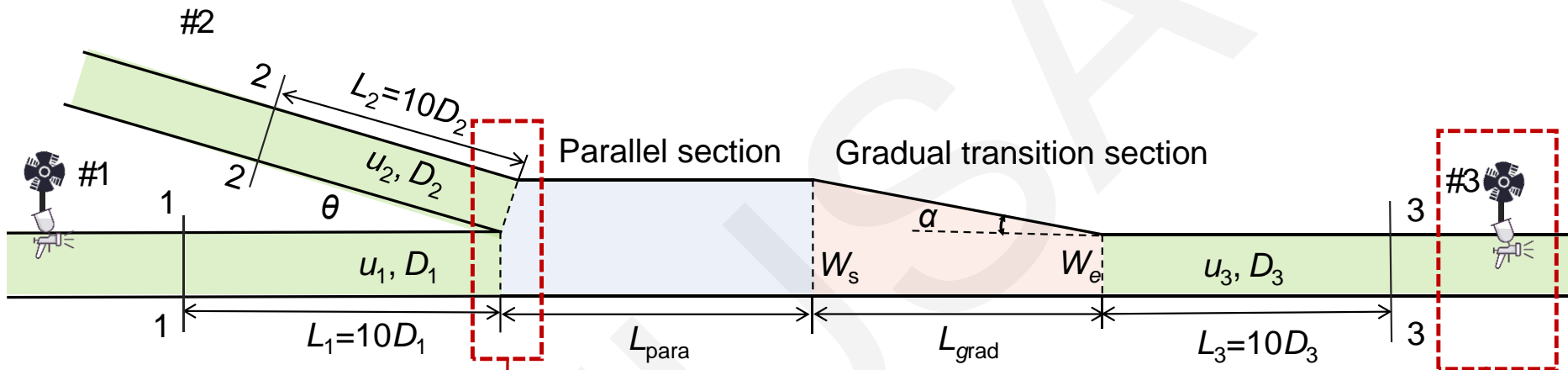


Fig. 2 Schematic diagram of tunnel bifurcation

# Experimental Setup



Confluence angle



Fig. 1 Ventilation scale model tunnel experimental platform for the bifurcation tunnel

# Effect of the confluence ratio $q$

## ■ Parallel Confluence Losses:

- Velocity Gradient Changes
- Streamline Curvature
- Flow Separation (Induced by Structural Abruptions & Jet Entrainment)

## ■ Flow Separation Location Features:

- $q \downarrow$ : at the upper part of the junction
- $q \uparrow$ : near the mainline side of the confluence section

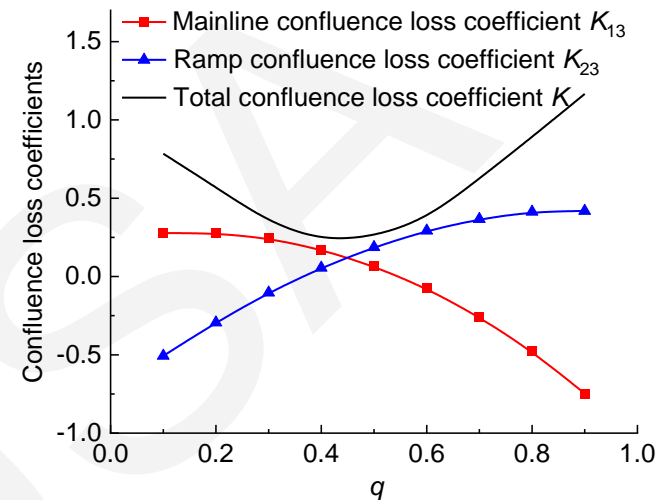


Fig. 3 Variation of the loss coefficients in the parallel confluence section

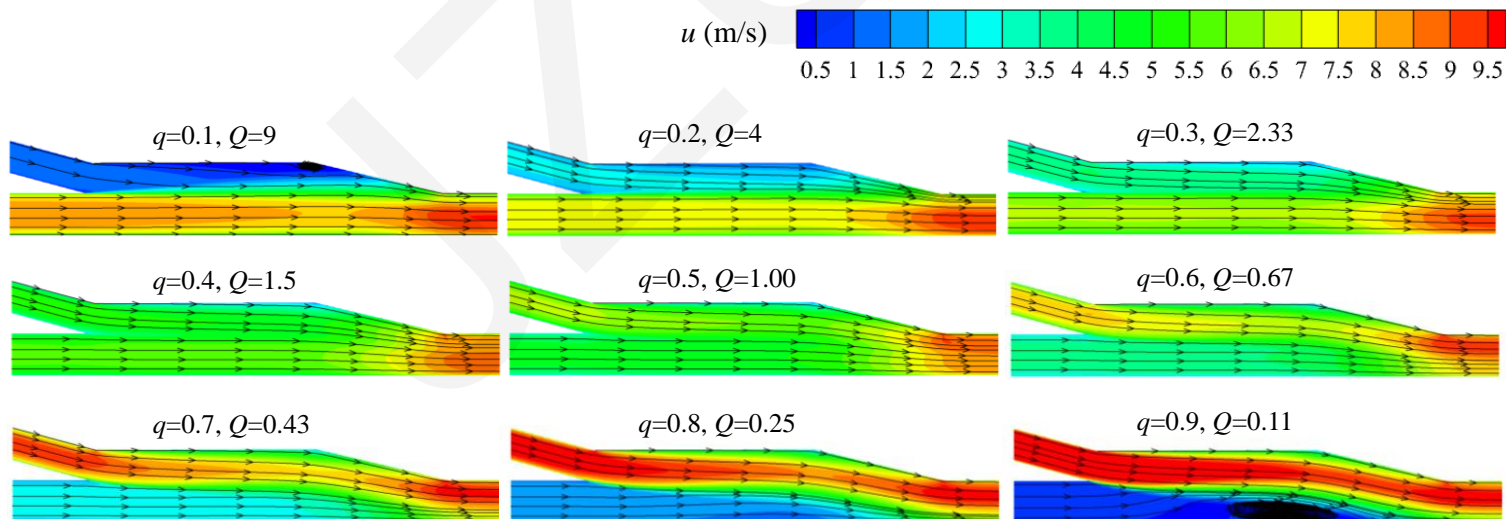


Fig. 4 Flow structure of the parallel confluence section at  $\theta = 15^\circ$

# The effect of the confluence angle $\theta$

- For small  $q$ :  $K$ ,  $|K_{13}|$  and  $|K_{23}|$  are almost unaffected by  $\theta$
- For large  $q$ :  $K$ ,  $|K_{13}|$  and  $|K_{23}|$  decrease with the increase of  $\theta$

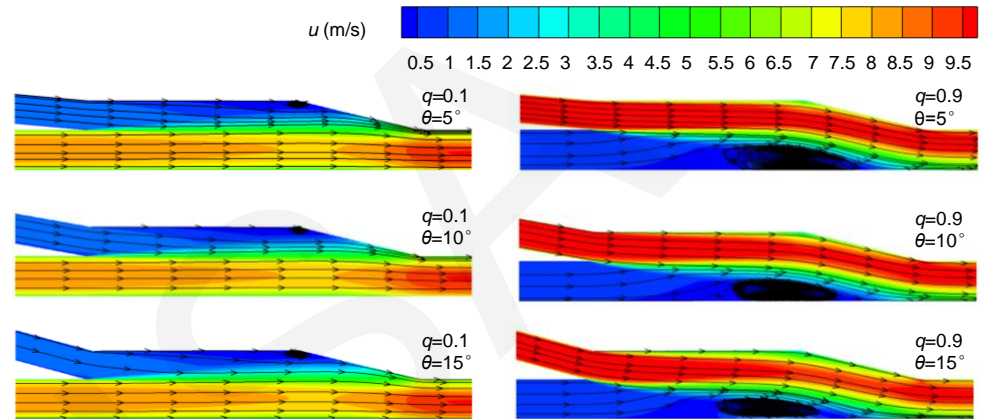


Fig. 7 Flow structure of the parallel confluence section

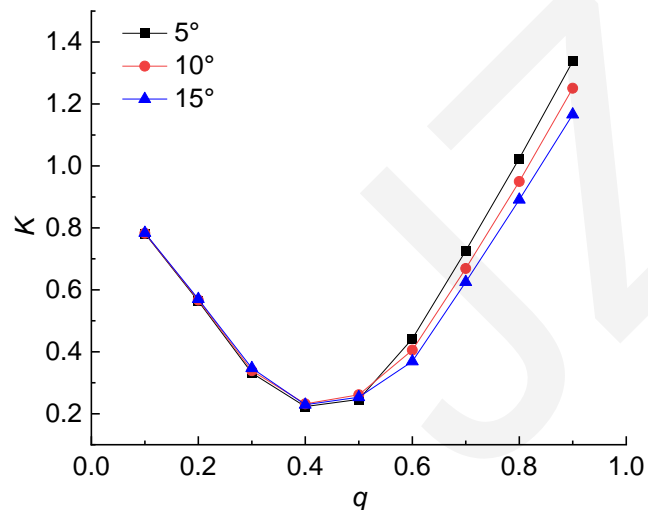


Fig. 5 Total loss coefficient in the parallel confluence section

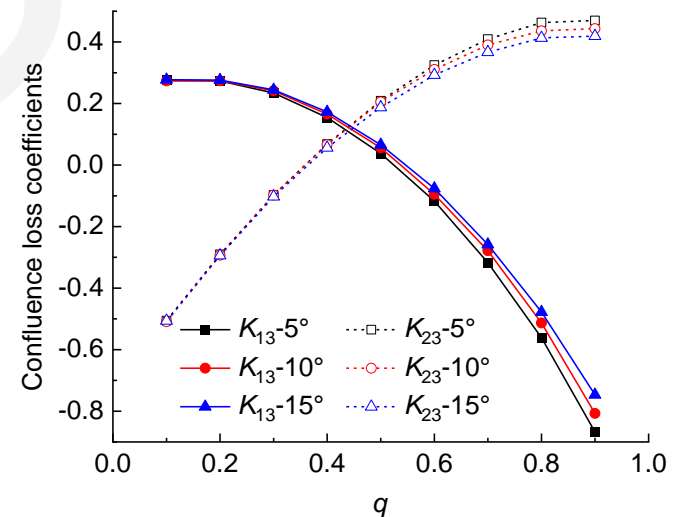


Fig. 6 Loss coefficients of the mainline and ramp in the parallel confluence section

# Predictive model of loss coefficients in the parallel confluence section

$$K_{13} = \xi'_{13} + k(\xi_{\text{para}} + \xi_{\text{grad}})$$

$$K_{23} = \xi'_{23} + k(\xi_{\text{para}} + \xi_{\text{grad}})$$

$$\xi'_{13} = \frac{2\varphi \left[ 1 - (1-q)^2 - q^2 \varphi \cos \theta_{13} \right]}{\varphi + \frac{1}{2} \cos \theta_{13}} + (1-q)^2 - 1$$

$$\xi'_{23} = \frac{2\varphi \left[ 1 - (1-q)^2 - q^2 \varphi \cos \theta_{23} \right]}{\varphi + \frac{1}{2} \cos \theta_{23}} + q^2 \varphi^2 - 1$$

$$\theta_{13} = 17.31 + 4.535q - 1.168 + \theta$$

$$\theta_{23} = 41.32q - 0.498 - \theta - 23.62$$

- local loss of the flow field due to "sudden expansion-gradual contraction" effects

$$\xi_{\text{para}} = \lambda \frac{L_{\text{para}}}{D_{\text{para}}} \left( \frac{W_s}{W_e} \right)^2$$

$$\xi_{\text{grad}} = \frac{\lambda W_e^2}{2H \tan \alpha} \left[ H \left( \frac{1}{2W_e^2} - \frac{1}{2W_s^2} \right) + \left( \frac{1}{W_e} - \frac{1}{W_s} \right) \right]$$

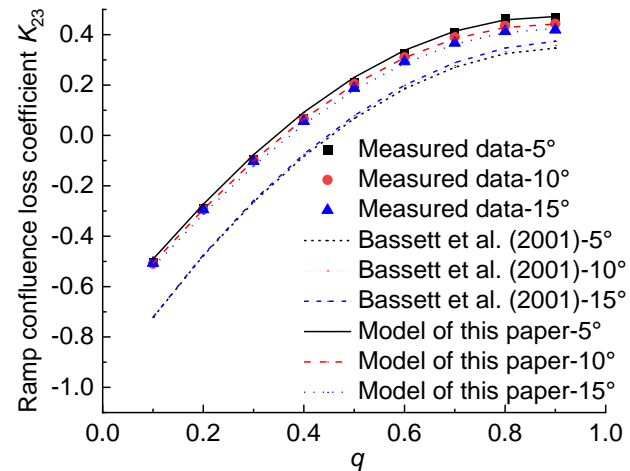
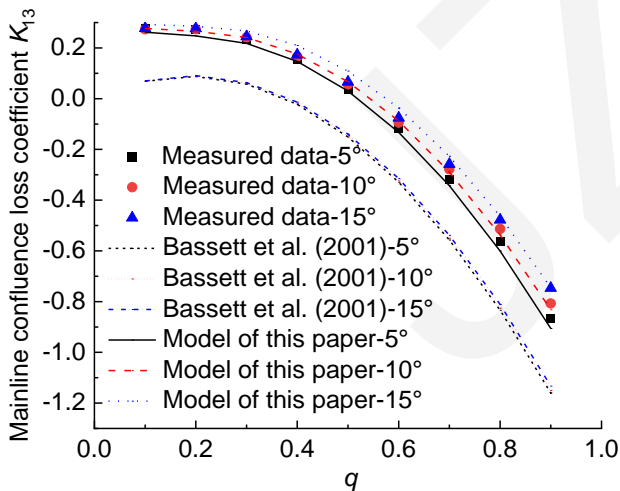


Fig. 7 Comparison of the proposed formula, Bassett's formula calculation results, and test results